

THE CORRELATION POTENTIAL OF MAGNETIC SUSCEPTIBILITY AND OUTCROP GAMMA-RAY LOGS AT TOURNAISIAN-VISÉAN BOUNDARY SECTIONS IN WESTERN EUROPE

Ondřej BÁBEK^{1,2}, Jiří KALVODA¹, Markus ARETZ³, Patrick J. COSSEY⁴, François-Xavier DEVUYST⁵, Hans-Georg HERBIG⁶ & George SEVASTOPULO⁷

(10 figures)

¹*Department of Geological Sciences, Masaryk University, Kotlářská 2, 61137 Brno, Czech Republic, e-mail: babak@sci.muni.cz*

²*Department of Geology, Palacky University, Tř. 17. listopadu 12, 77146 Olomouc, Czech Republic*

³*Université de Toulouse (UPS), LMTG (OMP), CNRS, IRD, 14 avenue Edouard Belin, 31400 Toulouse, France*

⁴*Faculty of Science, Staffordshire University, College Road, Stoke-on-Trent, Staffordshire, ST4 2DE, United Kingdom*

⁵*Carmeuse Coordination Center, bd. de Lauzelles, 65, B-1348 Louvain-la-Neuve, Belgium*

⁶*Institut of Geology and Mineralogy, University of Cologne, Zulpicher Str. 49a, 50674 Cologne, Germany*

⁷*Department of Geology, Trinity College Dublin, Dublin 2, Ireland*

ABSTRACT. We have measured five deep-water carbonate and carbonate-siliciclastic sections at the Tournaisian-Viséan (Tn/V) boundary in western Europe, using petrophysical outcrop logging techniques (gamma-ray spectrometry /GRS/ and magnetic susceptibility /MS/). The aim was to trace correlatable log patterns across the flanks of the London-Brabant Massif from eastern Ireland to western Germany. Both GRS and MS logging proved useful for long-distance (up to ~1000 km) correlation. The log patterns can be interpreted in terms of sea-level fluctuations. A late Tournaisian regression, a sequence boundary at the Tn/V boundary, early Viséan lowstand systems tract and an overlying transgressive to regressive succession can be identified from the GRS and MS logs. The Tn/V sequence boundary can be correlated with exposure features and karstic surfaces in the up-dip shallow-water settings at the boundary between sequence 4 and 5 of Hance et al. (2001, 2002). This indicates that sea-level fluctuations around the Tn/V boundary were synchronous and traceable on the flanks of the London-Brabant Massif. The GRS-based logging has a greater correlation potential than MS as it can be applied in a broad spectrum of facies and depositional settings. In certain sections, the MS signal shows an increasing trend during transgression and a decreasing during regression, which is opposite to the MS paradigm from shallow-water carbonate platform settings. These trends are assumed to result from landward/basinward facies shifts of low-productivity carbonate ramp systems. Lowstand shedding of carbonate tempestites and turbidites results in low MS values while during sea-level rise the ramp systems backstep, developing retrograding facies successions in their distal parts, which are associated with upward-increasing MS values.

KEYWORDS: Outcrop logging techniques, foraminifer biostratigraphy, Carboniferous, deep-marine sediments, sea-level changes

1. Introduction

The Tournaisian/Viséan (Tn/V) boundary interval represents a period of important sea level and oceanographic changes on a regional to global scale. In mostly shallow-water facies of Europe, the regional correlation is based on sequence stratigraphy, which is backed up by conodont and foraminifer biostratigraphy and microfacies analysis (Hance et al., 2001; Devuyt & Hance in Poty et al., 2006; Devuyt, 2006; Devuyt & Kalvoda, 2007). The Tn/V boundary around the London-Brabant Massif is associated with sea-level fall, which is documented by exposure features and karstic surfaces in shallow-water carbonate platforms (Faulkner et al., 1990; Hance et al., 2001; Devuyt, 2006). In the late Tournaisian to middle Viséan, synsedimentary tectonic activity and widespread extension are reported around the London-Brabant Massif (Ziegler, 1982; Leeder, 1987; Gawthorpe

et al., 1989; Fraser & Gawthorpe 1990; Nolan, 1989; Hance et al., 2001). Glacio-eustatic oscillations may also have played a role (Kalvoda, 2002) despite the fact that uncertainties still exist concerning the presence, distribution and extent of ice sheets in the Tournaisian and early Viséan (Devuyt, 2006).

However, the patterns of the sea-level fluctuation close to the Tn/V boundary are poorly constrained in deeper-marine facies. There are few papers attempting to interpret European deep-marine sections close to the Tn/V boundary in terms of sea-level fluctuations (Siegmond et al., 2002; Mottequin, 2008). In addition, the position of the Tn/V boundary may be difficult to locate with precision at times due to an absence of benthic foraminifers including the basal Viséan index species *Eoparastaffela simplex*. Consequently, the correlation between deep-marine sections at Tn/V boundary can be affected by a significant error. Petrophysical logs obtained from outcrop logging

may provide a suitable tool for correlation with much higher resolution than biostratigraphy. In particular, gamma-ray spectrometry (GRS), magnetic susceptibility (MS) logging or a combination of both has been used for correlation on the basin-wide scale (Doveton, 1994; Rider, 1999; Thibaut et al., 1999; Delius et al., 2001; Hladil et al., 2006; Da Silva et al., 2009; Whalen & Day, 2009; Koptíková et al., this volume). The spectral GR logs can be used for genetic interpretation of important stratigraphic surfaces such as condensed sections, flooding surfaces and sequence boundaries (Rider, 1999; Ehrenberg & Svana, 2001; Ruffel et al., 2004).

The GRS and MS logs bear additional compositional information related to the mineralogy and chemistry of sediment, which can be interpreted in terms of compositional variations, and used as a proxy for organic carbon, weathering regimes in source areas and modal composition of detrital grains (Rider, 1999; Ruffel & Worden, 2000; Zhang et al., 2000; Lüning et al., 2004; Takano et al., 2004). In this study, we present the results of GRS and MS logging of the generally uninterrupted, deep-marine Tn/V boundary sections across western Europe. GRS and MS logs were obtained from a multitude of sedimentary environments including mixed carbonate-siliciclastic and carbonate slope deposits (Rush section, Dublin area, Ireland), carbonate turbidites (Brownend Quarry, Derbyshire, England; Zippenhaus, Rhenish Slate Mts., Germany) and deep-water peri-mudmound carbonates and shales (Sovet and Salet sections, Dinant synclinorium, Belgium). The objective was to (i) refine the (bio)stratigraphic resolution; (ii) expand the *Eoparastaffela*-based biostratigraphic correlation of Tn/V boundary to deep-marine facies where the index taxon may be absent; (iii) filter out local from regional/global steering mechanisms on deposition; and (iv) test the correlation potentials of GRS and MS outcrop logging.

2. Geological setting and biostratigraphy

2.1. Geological setting and location of the sections

All the localities occur in a rim around the structural high of the Caledonian London-Brabant Massif, a part of the former East Avalonia microcontinent (Ziegler, 1982; Bless et al., 1980; Krawczyk et al., 2008). The localities studied in Ireland (Rush, County Dublin) and England (Brownend, Staffordshire) are located on the northern flanks of the massif while the localities in Belgium (Salet and Sovet) and Germany (Zippenhaus) lie on the southern flank (Fig. 1).

The Rush coastal section is located on the eastern coast of Ireland close to the town of Rush, approximately 22 km NE of the centre of Dublin (WGS-84: 53°32'18"N; 6°4'32"W). Rush is located in the Dublin Basin which provides sections of the late Tournaisian (in a shelf/ramp setting) and all of the Viséan (in both basinal and shelf settings) (Sevastopulo & Wyse Jackson, 2008). The late Tournaisian Feltrim Limestone Formation consists of Waulsortian facies mudbank limestone, followed by basinal shales and limestones of the late Tournaisian Tober Colleen Formation (Sevastopulo & Wyse Jackson, 2008).

At that time, the Dublin Basin was definitely subsiding through fault displacements and there was a lithological contrast between shallow water carbonates on the Balbriggan Block to the north and basinal facies at Rush. The Tober Colleen Formation is succeeded by conglomerates, limestones, sandstones and shales of the Rush Conglomerate Formation, which contains shallow water faunas and littoral sand and pebbles derived by turbidite flows from the margins of the higher blocks (Marchant, 1978; Nolan, 1986; Sevastopulo & Wyse Jackson, 2008).

The Brownend Quarry is located near the village of Waterhouses, on the left side of A523 road from Leek to Ashbourne, Staffordshire, central England (WGS-84: 53°2'19"N; 6°4'52"W). The quarry is located in the North Staffordshire Basin, which is interpreted by Lee (1988) as a halfgraben. Sedimentation started here during the Late Devonian or Hastarian (Fig. 2) with a deposition of the alluvial Redhouse Sandstones overlain by shallow subtidal to supratidal Rue Hill Dolomite (Hastarian-early Ivorian), deep ramp Milldale Limestone Formation (Ivorian-Chadian) and bioclastic 'inter-reef' and turbiditic facies of the Viséan Hopedale and Ecton limestone formations (Gawthorpe et al., 1989; Cossey et al., 1995, 2004; Waters et al., 2009).

The Belgian localities of Salet and Sovet are located in the Namur-Dinant Basin on the southern flanks of the London-Brabant Massif. The Midi-Eifel major thrust zone separates the Namur and Dinant outcrop belts, once parts of the same depositional basin. The Sovet section, a parastratotype of the base of the Moliniacian substage, is located in the south-western part of the Condroz Sedimentation Area (CSA) which was a transitional zone between more proximal facies to the north (Namur Sedimentation Area) and basinal facies to the south (Dinant Sedimentation Area, DSA). The section is exposed in a railway cutting on the Ciney-Spontin line at the old Sovet railway station, about 2 km north of the village of Sovet, in the Bocq Valley of the Condroz area. The upper third of the section close to the Tn/V boundary has the coordinates WGS-84: 50°18'59.6"N; 5°2'3.8"E. The Salet road section, a stratotype for the base of the Moliniacian, is located in the DSA (Hance et al., 2002). The Salet section is located in a road cut near the village of Salet, on the western slopes of La Molinee River, about 2 km W of the city of Anhée, Belgium (WGS-84: 50°18'43.4"N; 4°49'51.8"E). A detailed sequence stratigraphic model for the Mississippian of the Namur-Dinant Basin was proposed by Hance et al. (2001) and Devuyt (2006). In the CSA area, outer ramp peri-Waulsortian facies of the Leffe Formation are overlain by latest Ivorian to Moliniacian platform slope facies of the Sovet Formation whereas, in the DSA, the late Ivorian - early Moliniacian outer ramp Leffe Formation is overlain by the Moliniacian restricted basinal facies of the Molinee Formation.

The Zippenhaus Sedimentation Area in the Velbert Anticline in Germany represents the transition from the shallow marine Carboniferous limestone facies of the

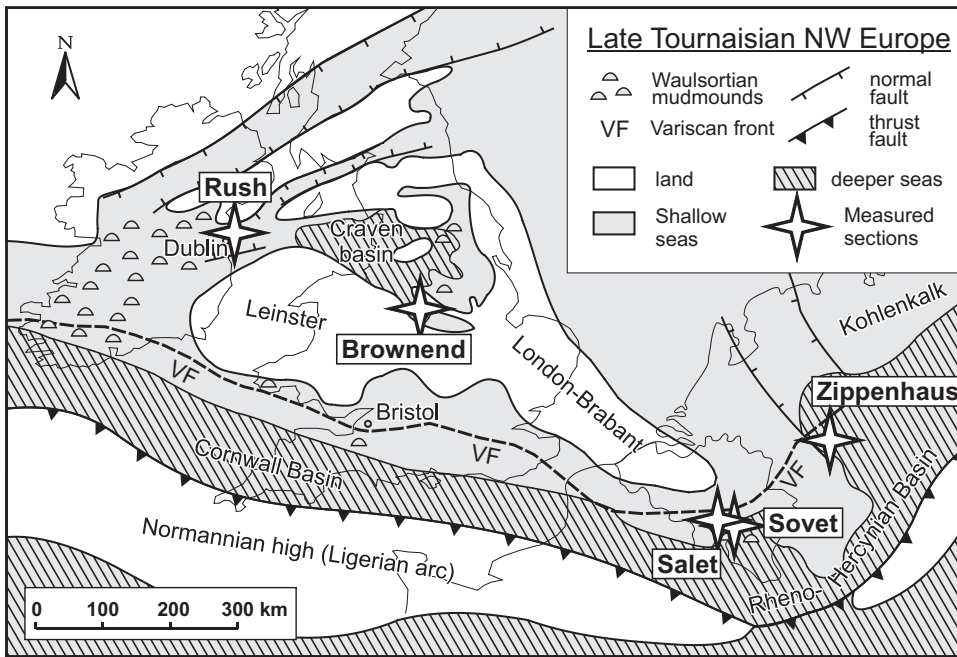


Figure 1. Late Tournaisian paleogeography of the London Brabant Massif with the position of the measured sections.

Namur-Dinant Basin to the deeper water facies of the Kulm Basin. The Zippenhaus section is located in an abandoned quarry in close proximity to Weilers Zippenhaus near Velbert, approximately 24 km ENE of the city centre of Düsseldorf, Germany (WGS-84: 51°20'4.4"N; 7°5'26.2"E). It comprises mainly calciturbidites, which alternate with Kulm-styled shaly sediments (Aretz et al.,

in print). Phosphate-bearing basinal black shales with limestone intercalations ("Liegender Alauschiefer") of the Hastarian age are in sharp contact with the overlying well-bedded basin slope carbonates of the Heiligenhausen Formation (Ivorian-Warnantian). The onset of Kulm-styled facies patterns is apparent in the latest Warnantian Dieken and Eisenberg formations.

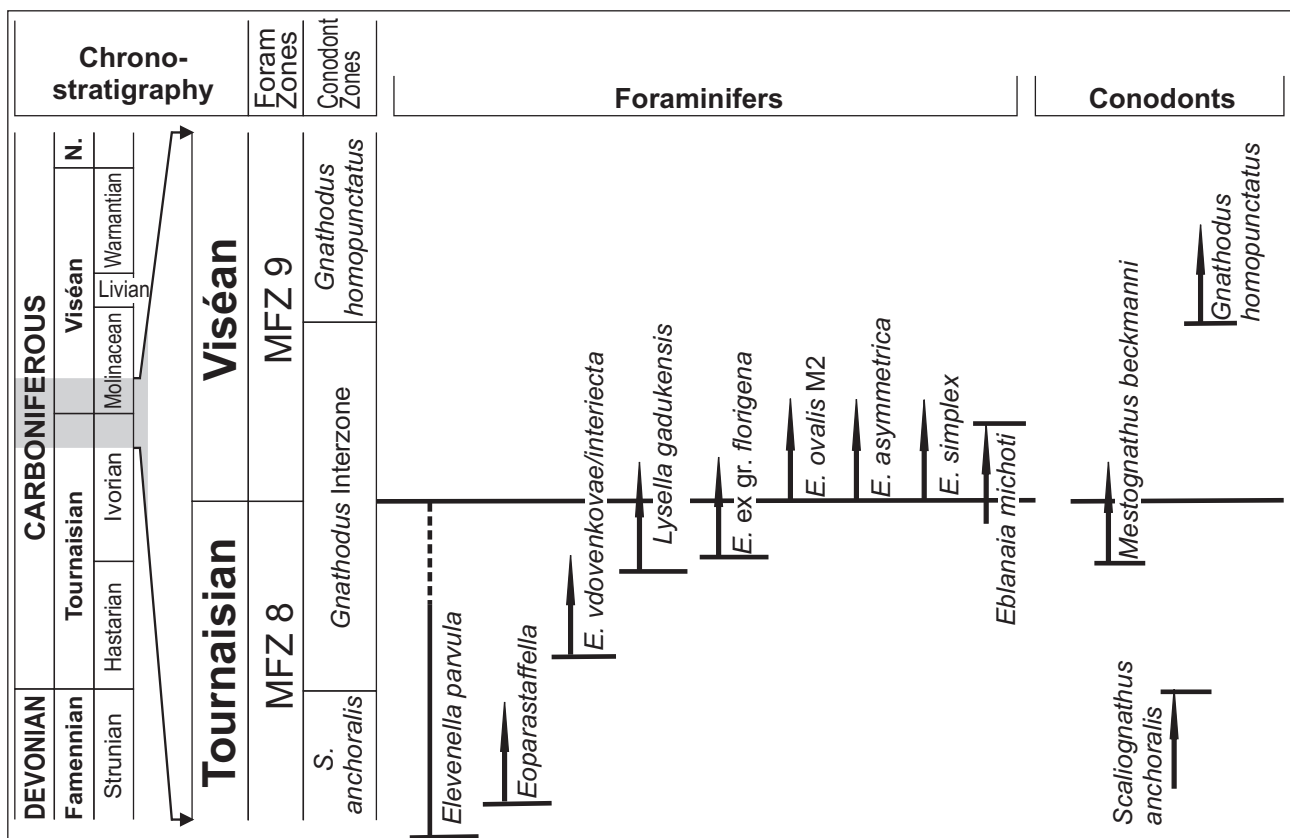


Figure 2. Important conodont and foraminifer biostratigraphic horizons close to the Tournaisian – Viséan boundary. Chronostratigraphic data adopted from Poty et al. (2006)

2.2. Important biostratigraphic index taxa close to the Tn/V boundary

The high-resolution biostratigraphy of the Tn/V boundary interval is primarily based on the foraminiferal fauna (Fig. 2). The search for a new stratotype for the base of the Viséan contributed to the substantial progress summarized in the foraminifer zonation by Devuyst and Hance (in Poty et al., 2006) and its subsequent refinements by Devuyst (2006) and Devuyst and Kalvoda (2007). The boundary is placed at the base of Zone 9 in the lineage from *Eoparastaffella ovalis* group to *Eoparastaffella simplex*. The base of Zone 8 coincides with the entry of the first fusulinid *Eoparastaffella*. Higher up in the zone, first appearance datum (FAD) of *Eoparastaffella vdoenkovae* and its closely related species *E. interiecta* and *E. macdermoti* (*Eoparastaffella* ex gr. *interiecta*), *Lysella gadukensis* and *Eoparastaffella* ex gr. *florigena* appear as particularly reliable biostratigraphic markers. The first *E. simplex* are not always very common and, in their absence, the entry of *Eoparastaffella ovalis* Morphotype 2 and *Eoparastaffella asymmetrica* represent important guides (Fig. 2) (Devuyst, 2006; Devuyst & Kalvoda, 2007). In the new Pengchong stratotype transitional forms between *E. ovalis* M2 and *E. simplex* occurs shortly before the first *Eoparastaffella simplex* (Devuyst, 2006). The disappearance of *Elevenella parvula* in late zone 8 or close to the Tn/V boundary represents another important event.

Among conodonts, the last appearance datum (LAD) of *Scaliognathus anchoralis* below the base of the Viséan represents the most reliable event that can be traced worldwide. The stratigraphic interval between the LAD of *S. anchoralis* and the FAD of *Gnathodus homopunctatus*, an index species of the first Viséan conodont zone, commonly contains abundant *Gnathodus* (in particular *G. pseudosemiglaber*) and was recently named the *Gnathodus* Interzone (Devuyst & Kalvoda, 2007). The appearance of *Mestognathus beckmanni* from its ancestor *M. praebeckmanni* slightly below the Tn/V boundary represents another very useful level (Fig. 2).

3. Material and methods

Bed-by-bed logging with field description of bed thickness, bed geometry, grain size and sedimentary structures was performed at the Rush and Brownend sections. The logging data for the Sovet, Salet and Zippenhaus sections were adopted from Devuyst (2006), Amler and Herbig (2006) and Aretz et al., in print). In order to provide biostratigraphic control on the petrophysical logging, all the sections were sampled for foraminifer biostratigraphy. Additional biostratigraphic control was based on published conodont and foraminifer faunas.

The sections were logged for GRS using an Exploranium RS-230 Super Spec portable spectrometer with a 2x2" (103 ccm) bismuth-germanate (BGO) crystal detector (Radiation Solutions Inc., Canada). Counts per seconds in selected energy windows were directly converted to concentrations of K (%), U (ppm) and Th

(ppm). Depending on the total thickness, the logging interval was 0.25 (Zippenhaus), 0.5 (Brownend, Sovet, Salet) and 0.5 to 1.0 m (Rush) of thickness. One measurement with a 240-s count time was performed at each logging point, perpendicular to the section wall and at full contact with the rock. Detection limits are 0.1 % for K and 0.4 ppm for U and Th. The combined error from operating conditions, instrument and repeated measurements was estimated to be less than about $\pm 7.5\%$ for the K, U and Th concentrations. Six hundred and seventy six GRS data points (Rush: 288; Brownend: 132; Sovet: 127; Salet: 72; Zippenhaus: 57) were measured.

Fresh rock samples for bulk magnetic susceptibility (MS) measurement, weighing from 9.02 to 73.49 g were collected at 0.125 to 0.5 m spacing, depending on the total section thickness. MS was measured using KLY-4 kappabridge (Agico, Czech Republic; magnetic field intensity of 300 Am⁻¹, operating frequency of 920 Hz, sensitivity of 4.10⁻⁸ SI). Mass-specific MS data expressed in m³kg⁻¹ were used. A total of 659 MS samples (Rush: 288; Brownend: 128; Sovet: 123; Salet: 71; Zippenhaus: 49) were measured.

4. Results

4.1. Rush Section, eastern Ireland

4.1.1. Lithology, stacking patterns and biostratigraphy

The measured section is 192 m thick and comprises uppermost Tournaisian to lower Viséan sedimentary rocks. The basal part of the section (Fig. 3, 192 to 133 m below section top) comprises monotonous, dark-grey to black shales alternating with micritic argillaceous limestones with infrequent gastropods and nautiloids (Tober Coleen Formation). This part is interpreted as hemipelagic deposits. The overlying part (133 to 0 m) is composed of carbonate and siliciclastic-carbonate arenites alternating with shales, siltstones and siliciclastic-carbonate conglomerates and breccias (Rush Formation). The arenite beds are medium- to coarse-grained, typically 1 cm to ~1 m thick, normally graded, with sharp bases, parallel and wavy lamination, basal scours and shale intraclasts. The conglomerates and breccias are normally up to ~4 m thick, graded to non-graded, with outsized clasts, sometimes projecting above the bed tops, and are frequently associated with soft-sediment deformation beneath their bases (Fig. 3). This succession is interpreted as carbonate and siliciclastic-carbonate turbidites and sandy debris-flow beds deposited on the background of hemipelagic clayey and silty sedimentation (Sevastopulo & Wyse Jackson, 2008).

The Rush Formation starts with a thickening and coarsening-upward (CU) succession (133 to 104 m) of turbidites and sandy debris-flow beds, which is capped by two thick debris-flow breccias separated by coarse-grained and fine-grained turbidites (104 to 92 m). These debris-flow beds are ~3.5 m to ~5 m thick, inverse and/or normally graded and capped with graded, coarse-grained calcarenites (turbidite cap). In the overlying succession (92 to 52 m),

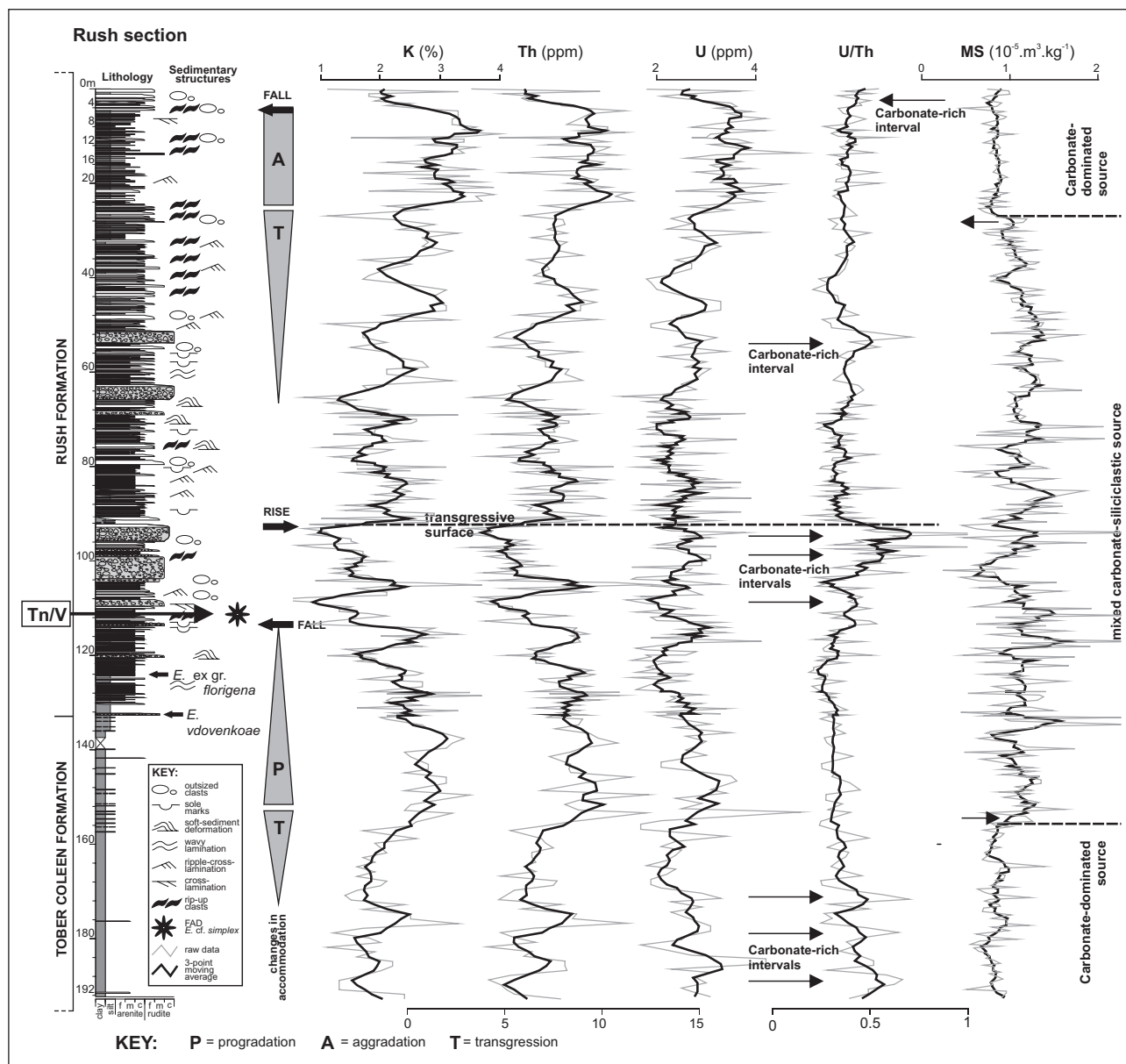


Figure 3. Lithology, lithostratigraphy, biostratigraphy and spectral gamma-ray- and magnetic susceptibility logs of the Rush section, Ireland.

shales and siltstones cyclically alternate with turbidites and debris-flow breccias with an overall 45 to 30 net-to-gross ratio. The top part of the section (52 to 5 m), comprising a fining- and thinning-upward succession of turbidites with upward-increasing proportion of shales (75 to 50 net-to-gross ratio at the top of this succession), is capped by thick-bedded turbidites and sandy debris-flow deposits (5 to 0 m).

The basal parts of the Rush Formation correspond to the latest Tournaisian as indicated by the FAD of *Eoparastaffella ex gr. interiecta* (upper part of MFZ8) followed by *Eoparastaffella ex gr. florigena* and *Lysella gadukensis*, which is suggestive of the very latest Tournaisian (Fig. 2). Higher up it presumably hosts the MFZ8/MFZ9 foraminifer zone boundary (Tn/V boundary) at ~116 m, which is indicated by the FAD of *Eoparastaffella cf. simplex* (Fig. 3).

4.1.2. Gamma-ray spectrometry

The GRS and MS logs are shown in Fig. 3. The correlation between the total gamma-ray value (dose rate, nGy.kg^{-1}) and K, Th and U concentrations (Fig. 4), respectively, indicate that a major contribution to the total gamma-ray signal comes from potassium ($R^2 = 0.92$), followed by Th ($R^2 = 0.51$) and U ($R^2 = 0.36$). The GRS logs show a high degree of vertical organization. The hemipelagic shales and limestones at the base of the section (192 to ~156 m) are characterized by moderately high concentrations of K, U and Th, which show a cyclic arrangement. From the strong positive correlation between potassium and thorium ($R^2 = 0.83$) we can infer that the K and Th variation is primarily driven by the dilution effect of carbonate in this predominantly shaly succession. At ~156 m depth, there is a prominent increase in the concentrations of the K, U, Th and MS values, which remain high (K: ~3.1 %, Th: ~9

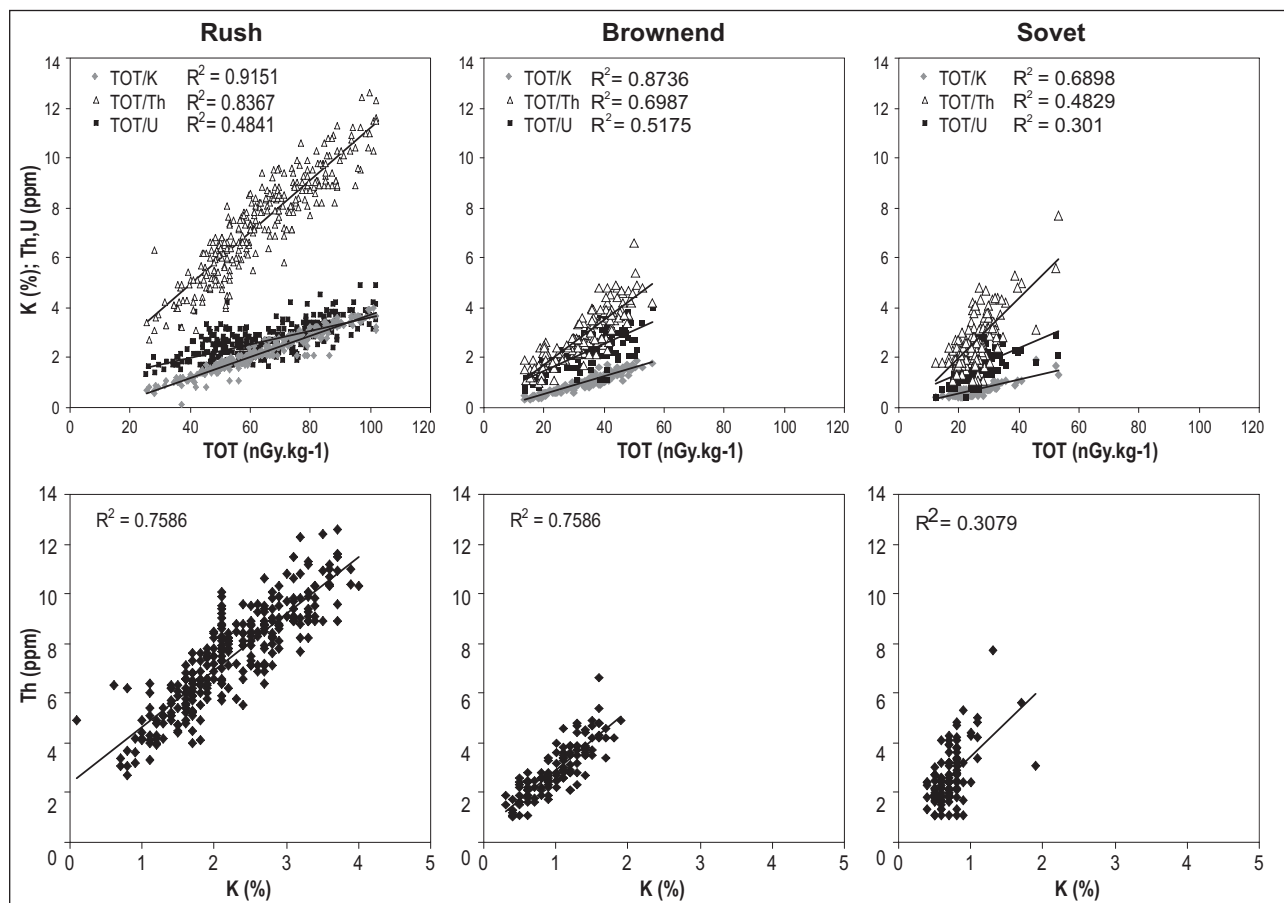


Figure 4. Bivariate plots and linear regression coefficients for total gamma-ray (dose rate, nGy.kg^{-1}) vs. K, Th and U concentration for the Rush, Brownend and Sovet sections (above). High correlation coefficients suggest the main sources of rock radioactivity (generally, Th and K). K/Th plots for the same sections below. High correlation coefficients indicate the dilution effect of non-radioactive components (mainly carbonate and quartz) in radioactive components (mainly clay minerals).

ppm, U: ~ 3.5 ppm; MS: $\sim 12.1 \times 10^{-6}$) up to the base of the Rush formation at ~ 133 m depth. Associated mainly with shales, this peak GRS signal is suggestive of a maximum coastal shift of facies. The base of the Rush Formation is represented by a decreasing trend in the GRS signal ending up in a particularly low concentration of K (~ 1.3 %) and Th (~ 4.8 %) in the coarse-grained turbidites and debris-flow breccias between ~ 92 and ~ 115 m. The base of this interval (~ 116 to ~ 115 m) coincides with the assumed position of the Tn/V boundary based on foraminifer faunas. This trend coincides with the CU trend in turbidite facies indicating overall progradation of the turbidite system during sea-level lowstand.

An abrupt increase in K and Th concentrations at 92 m depth, associated with a facies shift to a shale-rich interval, is suggestive of a transgressive surface. This surface separates the K and Th logs into a lower, generally prograding section and an upper, generally transgressive section. The surface is followed by two K and Th cycles, which coincide with two CU facies trends ending up in debris-flow breccias, between 92 and 63 m and between 63 and 51 m. Higher values of uranium normalized to thorium (U/Th ratios) in shaly interval at ~ 81 m depth are then suggestive of a local condensed horizon. Between 51 m and 24 m depth, the K and Th logs show increasing

values, which are followed by maximum K and Th concentrations between 24 and 4 m (mean K: $\bar{\emptyset}$ 3.2; mean Th: $\bar{\emptyset}$ 9.3). Being associated with a fining-upward facies tract, these log trends are suggestive of a major transgression followed by sea-level highstand conditions. In this interval, however, the Th and K logs reveal a hierarchic pattern with minor cycles superimposed on the major trends. Another major drop in K and Th concentrations occurs at ~ 4 m depth indicating a regressive surface. The U/Th ratio is low (0.25 to 0.45) throughout the Rush formation, apart from several minor peaks coinciding with low K and Th concentrations and carbonate-rich breccias where the U/Th ratio varies between 0.5 and 1. In such examples, the higher U/Th ratios are assumed to indicate a carbonate-rich lithology rather than condensation.

4.1.3. Magnetic susceptibility

MS values are low and uniform in the hemipelagic shales and marls of the Tober Coleen formation (Fig. 3; 4.8 to 11.9×10^{-6} ; $\bar{\emptyset}$ 8.4×10^{-6} ; standard deviation, σ : 1.5×10^{-6}). A progressive shift from lower to higher MS values occurs at ~ 156 m, which coincides with the increase in K and Th concentrations during maximum transgression. MS values are relatively high and highly variable in the top parts of

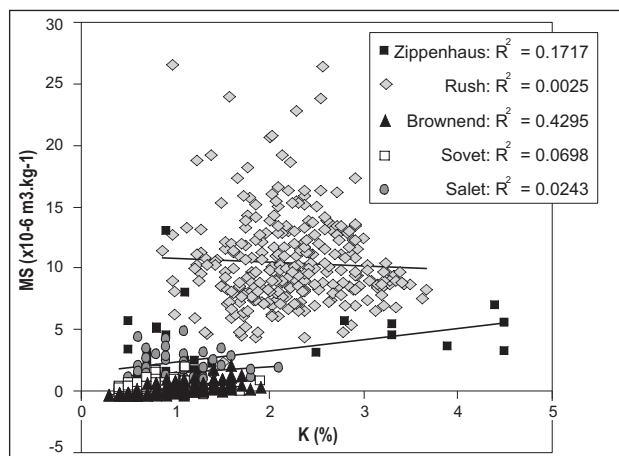


Figure 5. Bivariate plots and linear correlation coefficients for K concentrations vs. magnetic susceptibility for all the studied sections. Higher correlation coefficients (Brownend) suggest similar sources for rock radioactivity and magnetic susceptibility (e.g. dilution effect of siliciclastic admixture in carbonates); low correlation coefficients (e.g. Salet and Sovet) suggest different sources for both variables..

the Tober Coleen Formation and the Rush Formation between ~156 and ~28 m depth (2.3 to 26.5×10^{-6} ; σ 11.3×10^{-6} ; σ : 3.4×10^{-6}). This figure is at approximately an order of magnitude higher than in the carbonate-dominated sections such as Brownend (see below) where the MS values are low and correlated with the K signal (Fig. 5). The MS values decrease up-section between 51 and 24 m depth where K and Th concentrations tend to increase and sediment grain-size tends to decrease (Fig. 3). MS values consequently remain low and constant in the upper part of the section where K, U and Th reach maximum concentrations.

4.2. Brownend section, central England

4.2.1. Lithology and biostratigraphy

The measured section in Brownend is ~65 m thick and comprises uppermost Tournaisian to lower Viséan carbonates of the Milldale and Hopedale formations. The basal part of the section (65 to 47 m below section top) comprises graded, sometimes amalgamated, coarse-grained bioclastic turbidites (calcarenites to calcirudites) with abundant echinoderms, corals and brachiopods and

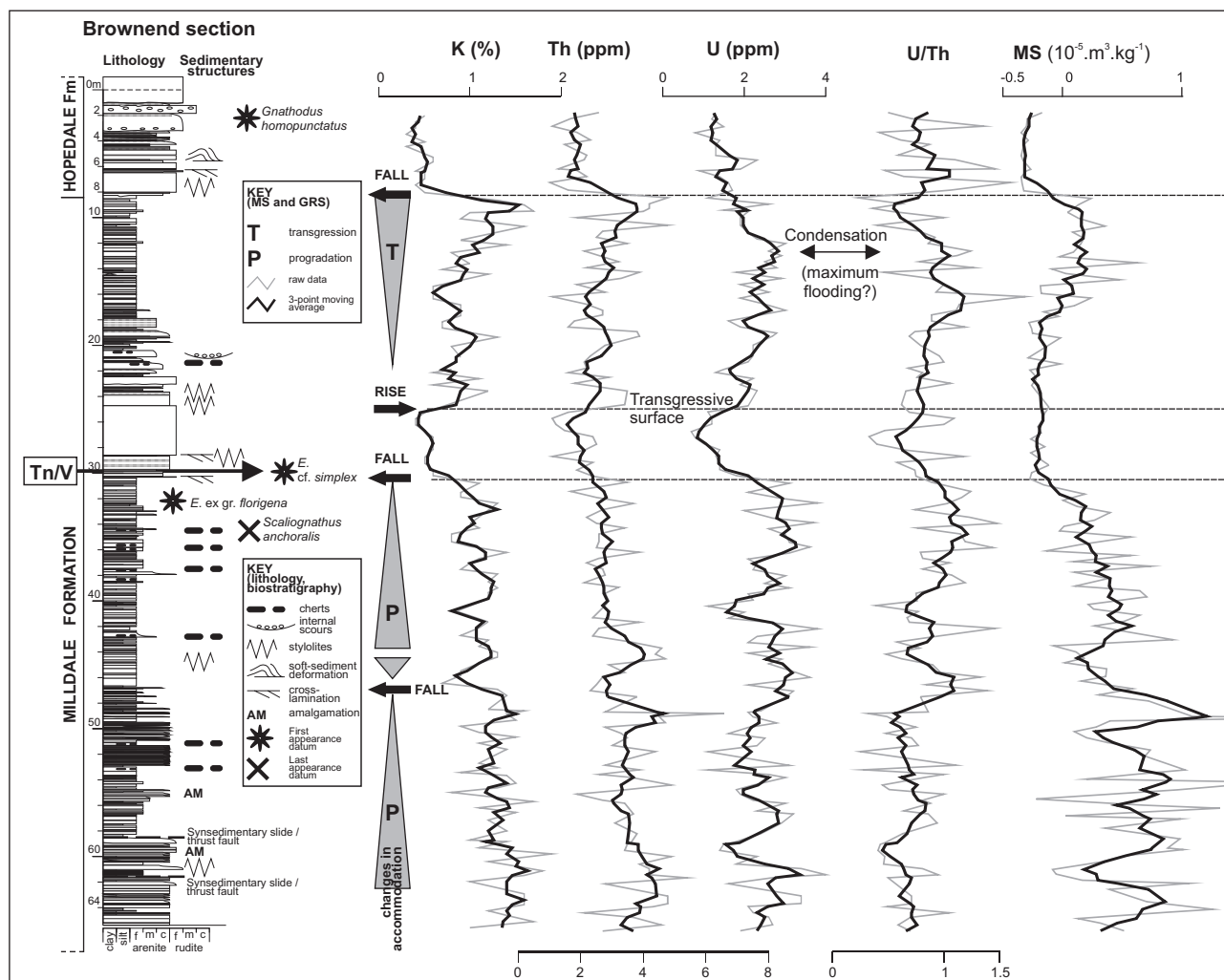


Figure 6. Lithology, lithostratigraphy, biostratigraphy and spectral gamma-ray- and magnetic susceptibility logs of the Brownend section, England.

frequent *Zoophycos* trace fossils, which alternate with grey to reddish marls (Milldale Formation). They are overlain by a coarsening-upward succession (47 to 30 m) of calcisiltites to fine-grained calcarenites with chert nodules, alternating with thin marl interlayers and scarce graded crinoidal calciturbidite beds (Fig. 4). Above this succession, there is a sequence of very thick beds of coarse-grained calcarenites to fine calcirudites (30 to 24 m), which is overlain by a fining-upward (FU) succession of graded and parallel-laminated carbonate turbidites (24 to 17 m) and finally by calcisiltites to fine-grained calcarenites with chert nodules and marl interlayers (17 to 8.5 m). The top part of the section (Hopedale Formation, 8.5 to 0 m) is represented by thick beds of coarse-grained, sometimes graded and parallel and/or cross-laminated calcarenites and carbonate breccias with abundant bioclasts and the FAD of *Gnathodus homopunctatus*.

The LAD of the upper Tournaisian index conodont species *Sc. anchoralis* lies approximately five metres below the coarse-grained calcarenites, in the middle parts of the section (~39 m). In the interval between 33 and 30 m, just below the coarse-grained calcarenites, the very latest Tournaisian (latest MFZ 8) *Eoparastaffella* ex gr. *florigena* and *Lysella gadukensis* is followed by FAD of *Eoparastaffella* cf. *simplex* (Fig. 4) which indicates the assumed Tn/V boundary.

4.2.2. Gamma-ray spectrometry and magnetic susceptibility

The GRS and MS logs are shown in Fig. 6. The K and Th concentrations are well correlated ($R^2 = 0.71$) and MS data, as well, are to a certain degree correlated with K ($R^2 = 0.43$) and Th ($R^2 = 0.32$) concentrations. The total gamma-ray signal is driven mainly by K ($R^2 = 0.87$) and Th (0.7) and, to a lesser extent, by U ($R^2 = 0.52$) (Fig. 4).

The basal part of the section (64.5 to 47 m below section top) shows high K and Th concentrations and generally high MS values (K: $\bar{\emptyset}$ 1.34 %; Th: $\bar{\emptyset}$ 3.74 ppm; MS: $\bar{\emptyset}$ 0.66×10^{-6}). The values are highly variable, which is likely related to the alternation of turbiditic and marly facies. After a short drop at ~47 m, there is a rise in K and Th concentrations between ~46 m and ~44 m depth, which is followed by an increase in MS values between ~44 m and ~43 m depth. The K and Th concentrations remain relatively high and stable and consequently decrease to reach distinct minima approximately at the Tn/V boundary (~30 to ~25 m, Fig. 6). The passage to the decreasing trend in K and Th at ~34 m is linked with relatively high U/Th ratios (Fig. 6). MS values show a systematically decreasing trend between ~44 and ~30 m. This decreasing trend is capped by an interval of low values of K, Th and MS between ~30 and ~25 m which coincide with the coarse-grained carbonate facies at the Tn/V boundary indicated by foraminifer biostratigraphy. There is a distinct rise in K, Th and U concentrations at the top of the coarse-grained calcarenites and calcirudites, at ~25 m. The Th and K concentrations consequently tend to increase up to the base of the calcarenites and breccias of the Hopedale

Formation (8.5 m) as does the MS, although with some delay (between ~22 and 8.5 m). This succession is regarded as generally transgressive (see chapter 5.1 below), which is well supported by facies data revealing the FU trend. This transgressive trend is interrupted by a prominent negative shift in K, Th concentrations and MS values at the base of the Hopedale Formation. The magnetic susceptibility log shape shows a good fit with the Th and K logs in the upper two thirds of the section (~47 m to the top) although the MS values are extremely low (-0.3 to 0.7×10^{-6}).

4.3. Sovet section, Dinant Synclinorium

4.3.1. Lithology and biostratigraphy

The measured section is 63 m thick (Fig. 7) and covers the carbonates of the Leffe Formation and lower parts of the Sovet Formation (beds # 20 to 145 of Devuyt, 2006). Lithologic and microscopic characteristics of the sections are adopted from Devuyt (2006). The basal part of the section comprises pale violet-grey calcilutite and very dark grey to black, argillaceous, organic-rich calcilutite to calcisiltite with frequent sponge spicules, ostracods, trilobites, fenestrate bryozoans and brachiopods (Leffe Formation, 63 to 20 m below section top). The dark grey calcilutites and calcisiltites constitute a homogeneous, 21.4 m-thick unit (61 to 40 m) close to the base of the section (Paire Member, Devuyt, 2006). Nodular to bedded, dark cherts are common in the lower part of this succession (~62 to ~38 m). The calcilutites of the upper part of Leffe Formation (~38 to ~20 m and in particular the interval between 24 and ~20 m) become strongly pseudo-nodular to pseudo-brecciated. The upper Tournaisian LAD of *Sc. anchoralis* is located within this succession, in bed 108 (Devuyt 2006). Macrofauna is virtually absent from the formation apart from the Paire Member, which contains heavily altered ostracods, ramose bryozoans, brachiopods and extremely abundant *Zoophycos* and *Chondrites* trace fossils. Carbonates of the Leffe Formation comprise suspension deposits and storm layers deposited in the outer- to mid ramp / slope environment, below the storm wave base (SWB), and partly under dysoxic bottom water conditions (Paire Member, Devuyt, 2006).

The basal part of the Sovet Formation (Calcaire de Sovet Member) is characterised by fine- to medium-grained dolomites alternating with bioclastic-crinoidal dolomites and limestones with moravamminid algae, brachiopods, ostracods and some foraminifers (mass-flow deposits and tempestites), capped by a remarkable mass-flow conglomerate (bed 118) with diverse limestone clasts in a medium- to coarse-grained dolomitic-oolitic matrix (Devuyt, 2006). The FAD of *Eoparastaffella ovalis* M3 in bed 115 (Devuyt, 2006) indicates a close proximity of the Tn/V boundary. The Tn/V boundary, inferred from the FAD of *Eoparastaffella ovalis* M2 and *Eoparastaffella* cf. *simplex*, correlates with the bed 118 (Devuyt, 2006). The overlying part is composed of dark-coloured, fine- to medium-grained oolitic tempestites, with occasional cross lamination and erosional scours (0 to 14.5 m).

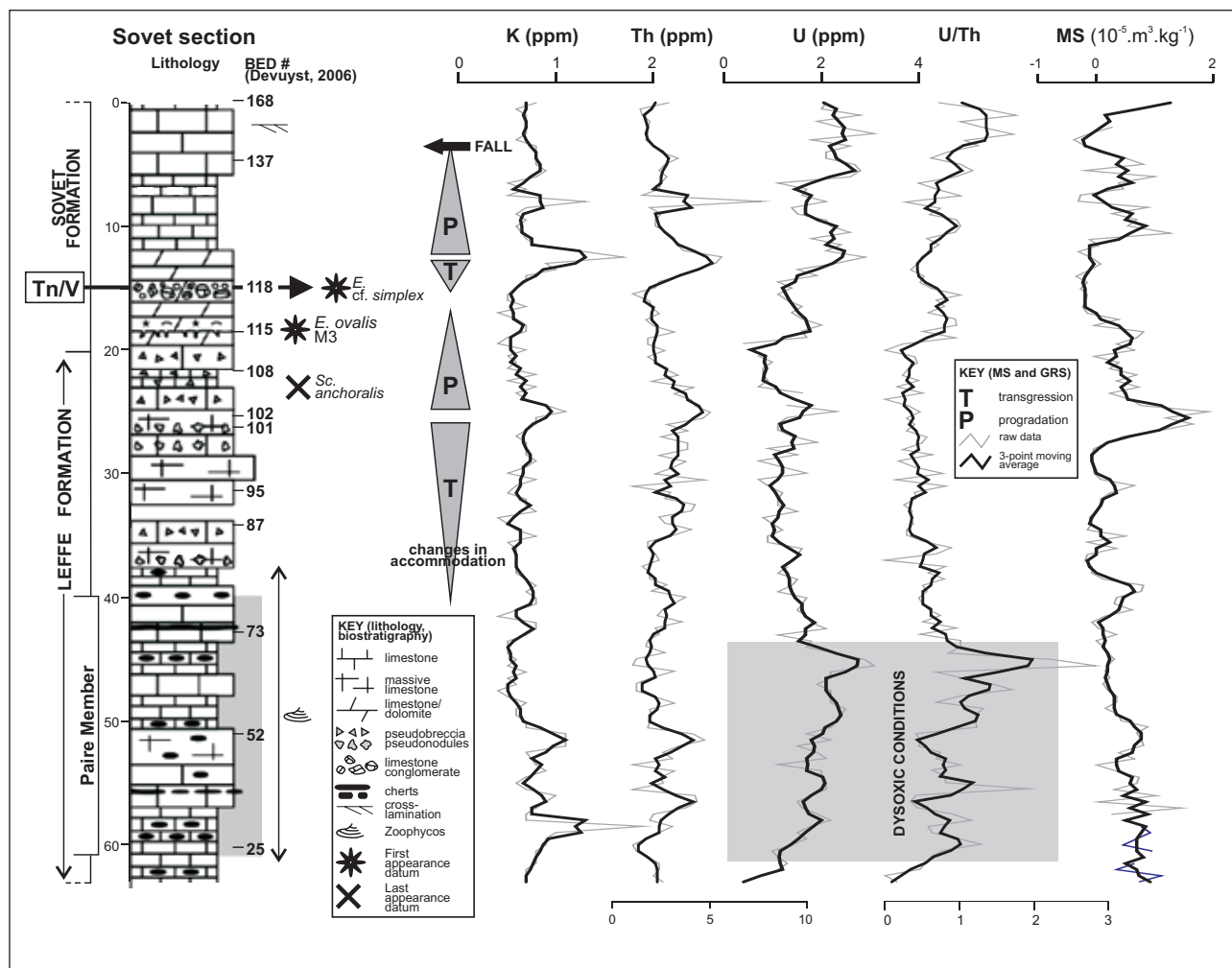


Figure 7. Lithology, lithostratigraphy, biostratigraphy and spectral gamma-ray- and magnetic susceptibility logs of the Sovet section, Belgium. Lithology log data adopted from Devuyt et al. (2006).

4.3.2. Gamma-ray spectrometry and magnetic susceptibility

The GRS and MS logs are shown in Fig. 7. Despite the overall carbonate-rich lithology, the K and Th concentrations are only poorly correlated ($R^2 = 0.31$) (Fig. 4). The major contribution to the total gamma-ray signal (TOT, given in dose rate, $\text{nGy}\cdot\text{kg}^{-1}$) is from potassium (TOT/K: $R^2 = 0.69$), followed by Th ($R^2 = 0.48$) and U ($R^2 = 0.3$) (Fig. 4). The MS data are not correlated with K ($R^2 = 0.07$; Fig. 5) and Th concentrations ($R^2 = 0.01$).

While being highly variable in the lower part of the Leffe Formation (63 to ~44 m), the K and Th concentrations tend to increase systematically between ~44 and ~25 m, reaching a maximum in bed 102 (25 m). These peaks coincide with peak U concentrations and peak MS values. The K and T concentrations and MS values consequently systematically decrease towards the mass flow breccias at the base of the Sovet Formation (bed 118; 15 m) while K/Th ratios tend to increase in the same interval. This situation is suggestive of a transgressive - regressive trend, which culminates close to 25 m below the section top (Fig. 7). This GRS and MS log section coincides with

the transgressive and highstand system tracts of sequence 4 of Devuyt (2006) inferred from detailed microfacies data. The GRS patterns (concentrations of K and Th) in bed 102 separate an underlying transgressive succession from an overlying regressive one (Fig. 7). A maximum regression is achieved in the succession with omission surfaces and mass-flow breccias (beds 115 and 118) as indicated by the lowest K and Th concentrations and low MS values and a local peak in U/Th ratios. The Tn/V boundary is placed here according to the foraminifer biostratigraphy. The K, Th and U concentrations consequently quickly increase to reach another prominent peak about 2 m above bed 118 (transgressive surface?). The rise in K and Th concentrations coincides with a prominent drop in K/Th ratios (not shown in the figure). The MS curve is dissimilar to the K and Th log patterns in the same interval but there is a prominent zone of low MS values between 17 and 11.5 m, associated with the mass-flow breccias and overlying dolomites (Devuyt, 2006). All of these prominent GRS and MS log patterns are located close to bed 118, which, according to Devuyt (2006) represents a sequence boundary coinciding with the Tn/V stage boundary. Towards the top of the section,

between 11.5 and 4 m, the K and Th values decrease, with local peaks, towards low values at the top of the section (4 to 0 m). The trends in the MS log are clearly independent of K and Th in the same interval.

4.4. Salet section, Dinant Synclinorium

4.4.1. Lithology and biostratigraphy

The measured section is ~36 m thick and comprises carbonates of the Leffe Formation (beds # 30 to 157 of Devuyst et al., 2006). The Leffe Formation consists of dark-grey to violet-grey lime mudstones and wackestones, sometimes laminated, commonly cherty and almost devoid of macrofauna. They were deposited from fine-grained carbonate suspension winnowed from Waulsortian mudmound facies (Devuyst et al., 2006). These suspension deposits are interlayered with distal storm beds. The upper Tournaisian LAD of *Sc. anchoralis* correlates with bed 52 in the lower third of the section (27.5 m below the section top; Fig. 8). The biostratigraphic Tn/V boundary is located in bed 124, 10 m below the section top, as indicated by FAD of *E. simplex* (Devuyst et al., 2006).

4.4.2. Gamma-ray spectrometry and magnetic susceptibility

The GRS and MS logs are shown in Fig. 8. Although K and Th concentrations are well correlated ($R^2 = 0.75$), the MS data are not correlated with either K ($R^2 = 0.02$) or with Th concentrations ($R^2 < 0.01$). The total gamma-ray signal is driven mainly by K ($R^2 = 0.75$) and Th (0.75) and, to a lesser extent, by U ($R^2 = 0.68$).

The concentrations of K and Th are variable in the lower part of the section until reaching a distinct minimum in the interval between ~22 and ~14 m below the section top. The LAD of *Sc. anchoralis* lies below this zone of low K and Th concentrations. This zone is associated with a peak in U/Th ratios (~17 to ~22 m) and, surprisingly a peak in MS values (~16 m). The K and Th then increases to reach the highest values at ~11 m depth, correlated with increasing U concentrations and decreasing U/Th ratios. This pattern is followed by decreasing trends in K and Th concentrations and increasing U/Th ratios towards the top of the section. The FAD of *E. simplex* is located at this level (~10 m).

The K, Th and U/Th log patterns make it possible to correlate the Salet section with the succession below and above the Tn/V boundary in Sovet. Similar to Sovet, the GRS variation can be interpreted in terms of transgressive-regressive trends. However, with respect to the common GRS log patterns at the Tn/V boundary, the biostratigraphic Tn/V boundary in Salet is located about 3.5 m higher than in Sovet. Despite the obvious uncertainty, it is assumed that the unfavourable (foraminifer poor) facies in Salet may have provided a poor basis for a reliable biostratigraphic correlation. The GRS log based correlation is therefore preferred. There also is a strong dissimilarity between the MS curves in both sections. MS values in Salet ($\bar{\varnothing} 1.5 \times 10^{-6}$) are distinctly higher than in Sovet ($\bar{\varnothing} 0.34 \times 10^{-6}$) and the MS signal fails to correspond with K and Th concentrations in both sections.

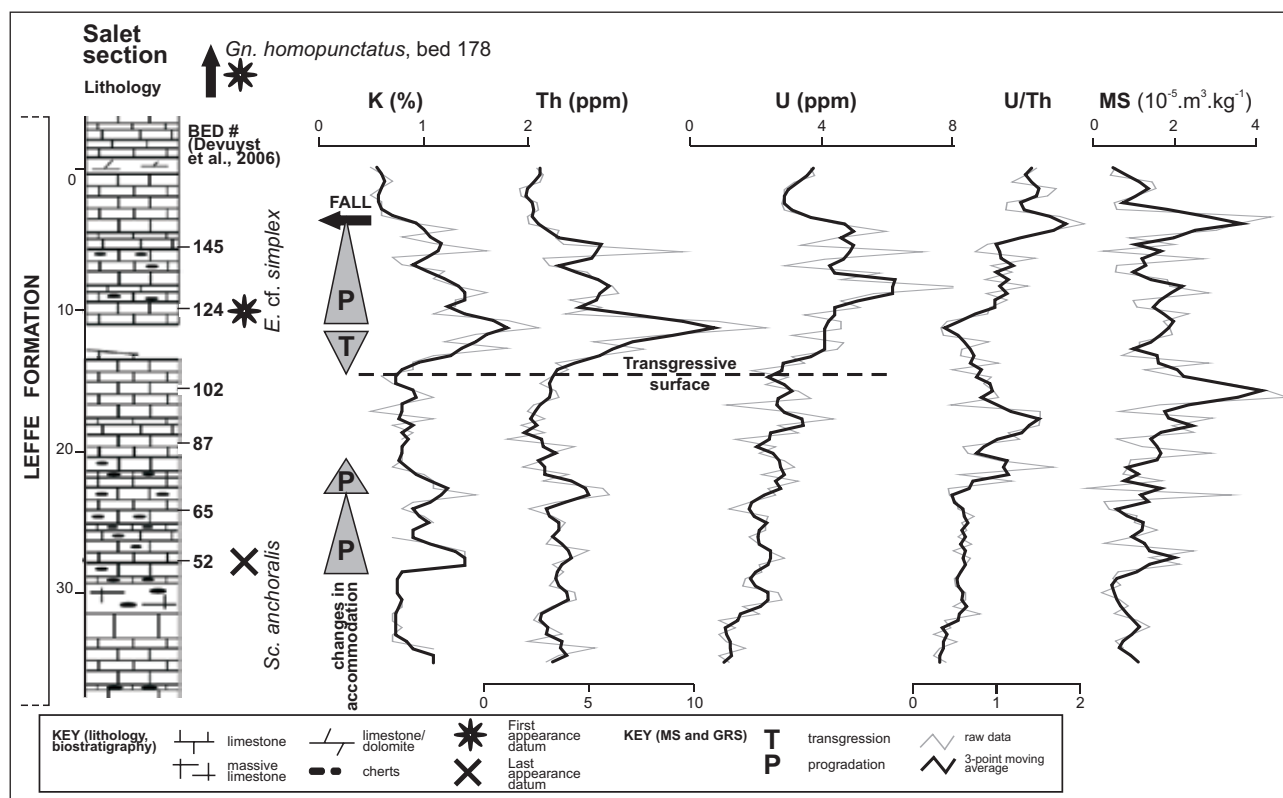


Figure 8. Lithology, lithostratigraphy, biostratigraphy and spectral gamma-ray- and magnetic susceptibility logs of the Salet section, Belgium. Lithology log data adopted from Devuyst et al. (2006).

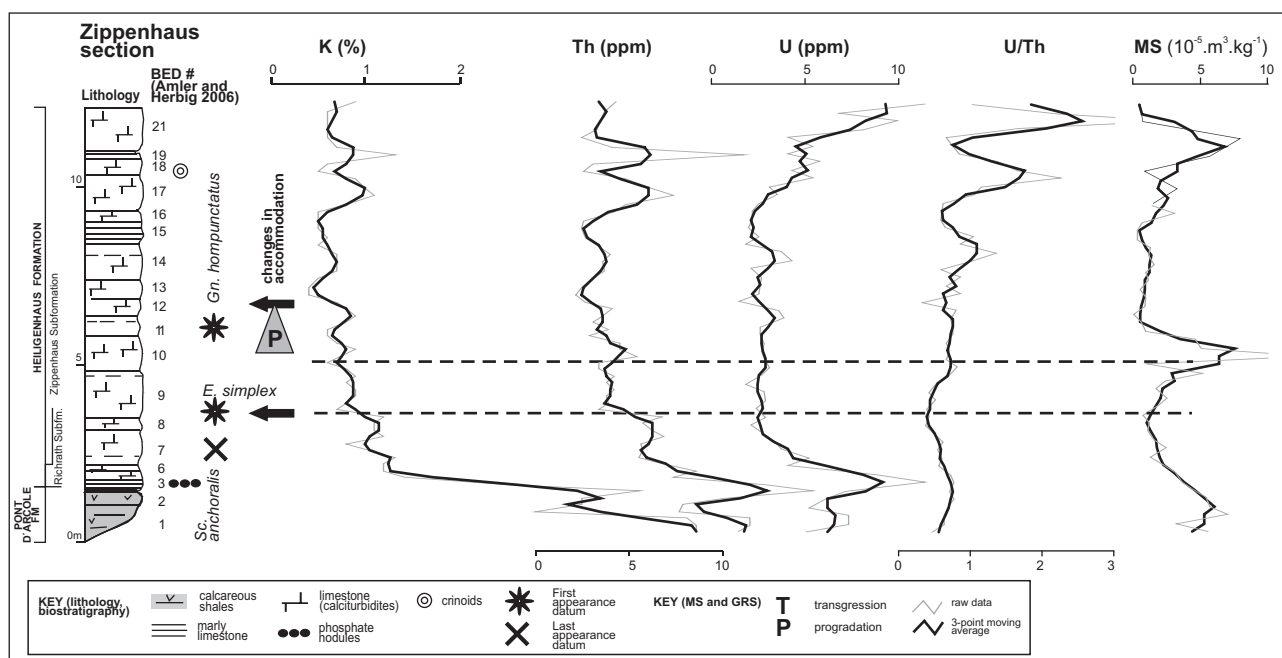


Figure 9. Lithology, lithostratigraphy, biostratigraphy and spectral gamma-ray- and magnetic susceptibility logs of the Zippenhaus section, Germany.

4.5. Zippenhaus, Rhenish Slate Mts.

4.5.1 Lithology and biostratigraphy

The measured section is ~12 m thick (Fig. 9) and comprises black shales of the Pont d'Arcole Formation and carbonates of the Heiligenhaus Formation (Richrath and Zippenhaus Subformations, Amler & Herbig, 2006). The black shales at the base of the section (0 to 1.5 m above section base, Pont d'Arcole Formation) are overlain by dark-grey, fine-grained, bituminous limestones with phosphate concretions (1.5 to 2.2 m, Richrath Subformation) and finally by well-bedded bioclastic, oolitic and peloidal, partly dolomitised and silicified calciturbidites (2.2 to section top, Zippenhaus Subformation). The LAD of *Sc. anchoralis* lies close to the base of the Zippenhaus Subformation (bed 7; 2.6 m above the section base). The Tn/V boundary, as indicated by the FAD of *E. simplex*, is located just ~1.2 m higher (base of bed 9; 3.8 m). The FAD of *Gn. homopunctatus* is located in bed 11 (6 m above section base). A very condensed succession is therefore inferred for the Tn/V boundary interval from these biostratigraphic data.

4.5.2. Gamma-ray spectrometry and magnetic susceptibility

The GRS and MS logs are shown in Fig. 9. If we put aside the black shales at the base of the section, the K and Th concentrations in the carbonates are correlated ($R^2 = 0.75$). The total gamma-ray signal is driven mainly by Th (0.85) and K ($R^2 = 0.81$) and, to a lesser extent, by U ($R^2 = 0.69$). However, the MS data are not correlated with K ($R^2 = 0.17$; Fig. 5) and Th concentrations ($R^2 < 0.12$).

Consistent with their lithology, the shales of the Pont d'Arcole Formation have high K and Th concentrations but relatively low U/Th ratios (< 0.8). The transition to the

overlying carbonate succession is accompanied by a drop in K, Th and U contents and a moderate drop to even lower U/Th ratios. The basal, upper Tournaisian succession of the Heiligenhaus Formation still has moderately high K (~1.1), Th (~6) concentrations, and low U/Th ratios. The Tn/V boundary (FAD of *E. simplex*) at the base of bed 9 is associated with another drop in K (~0.8) and especially Th (~4) contents. This pattern, although weak, is correlatable with Brownend, Rush and, to a lesser extent, Salet and Sovet, where the Tn/V boundary is associated with a drop or a distinct minimum of K and Th concentrations. The GRS signal in the overlying carbonates generally decreases up to bed 13 (7 m) although there are isolated peaks at certain levels. This is suggestive of an overall progradation. The base of bed 13 coincides with another significant drop in GRS values, which is suggestive of a basinward facies shift. It can be correlated with the previous sections, but its position above the FAD of *Gnathodus homopunctatus* points to an extreme condensation, which makes such an interpretation difficult. Between beds 13 and 20 (7 to 11 m), the concentrations of K, Th slowly increase with two positive excursions located in beds 17 and 20. The U concentrations increase more gradually to reach a distinct peak in bed 21 at the top of the section (11 to 12 m). The MS log shows trends which are dissimilar to the GRS log shapes (Fig. 9). In the lower parts of the section, the MS values decrease from the Pont d'Arcole shales to reach a distinct minimum at the Tn/V boundary (base of bed 9). The MS signal then increases up-section to reach a distinct positive peak in bed 10, still below the FAD of *Gn. homopunctatus*. This peak partly correlates with an increase in Th concentrations, which may suggest an increase in the fine-grained siliciclastic fraction (see below). However, for a carbonate lithology,

the MS values are high ($>10 \times 10^{-6}$), which suggests the MS signal can be influenced by ferromagnetic minerals. Consistent with the Brownend and Sovet MS signal, the Tn/V boundary is associated with a prominent depression on the MS log.

5. Discussion

5.1 GRS log correlation and sequence stratigraphic interpretation

From the GRS data correlation (Fig. 4), we can assume that the total gamma-ray activity in most of the sections is driven by potassium ($R^2 = 0.69$ to 0.92) and thorium ($R^2 = 0.48$ to 0.84) and, to a lesser extent, by uranium ($R^2 = 0.30$ to 0.69). The K and Th concentration data show a strong correlation ($R^2 = 0.75$ to 0.76) in all sections apart from Sovet ($R^2 = 0.31$). The GRS concentrations of K and Th in carbonates are thought to be related to the concentration of siliciclastic components (illite and other clay minerals, micas, K-feldspars) while a solid correlation between K and Th is considered to reflect a fine-grained siliciclastic admixture in carbonate rocks (Rider, 1999; Doveton, 1994; Fiet & Gorin, 2000; Ehrenberg & Svana, 2001; Fabricius et al., 2003). The relationship between increasing K and Th concentrations and decreasing CaCO_3 contents in carbonates was recently confirmed by Koptíková et al. (2010). The concentrations of uranium, by contrast, usually relate to the presence of organic carbon and calcium phosphates while uranium has a very

heterogeneous distribution in sediments (Rider, 1999; Lüning et al., 2004). We consequently interpret the K and Th variability in the predominantly carbonate sections (Brownend, Sovet, Salet and Zippenhaus) as reflecting a dilution of fine-grained terrigenous material (mostly clay minerals) in carbonate due to a variation in carbonate productivity and/or siliciclastic input into the basin (Koptíková et al., 2010). In Rush, however, the published data (Devuyst, 2006; Sevastopulo & Wyse Jackson, 2006) and our own observations point to a significant coarse-grained siliciclastic admixture in arenites and rudites. The high K and Th concentrations are in accordance with the observed lithology and it is likely that they are also partly related to the coarse-grained siliciclastic fraction in sandstones and conglomerates (micas, K-feldspars and heavy minerals)

The K and Th trends coincide with the observed and published (Devuyst, 2006) facies trends (coarsening-upward, fining-upward) in Rush, Brownend and Sovet, indicating that they are presumably related to landward (transgression) and basinward (progradation) facies shifts. The K, Th and total GR (dose rate) trends close to the Tn/V boundary are correlatable between most of the sections (Figs 3, 6, 7, 8, 9 and 10).

The total GR signal and in particular the Th concentrations gradually decrease up-section towards the Tn/V boundary in all the measured sections, most distinctly in Rush, Brownend, Sovet and Zippenhaus (Figs 3, 4, 5, 7 and 8). These trends coincide with the CU facies

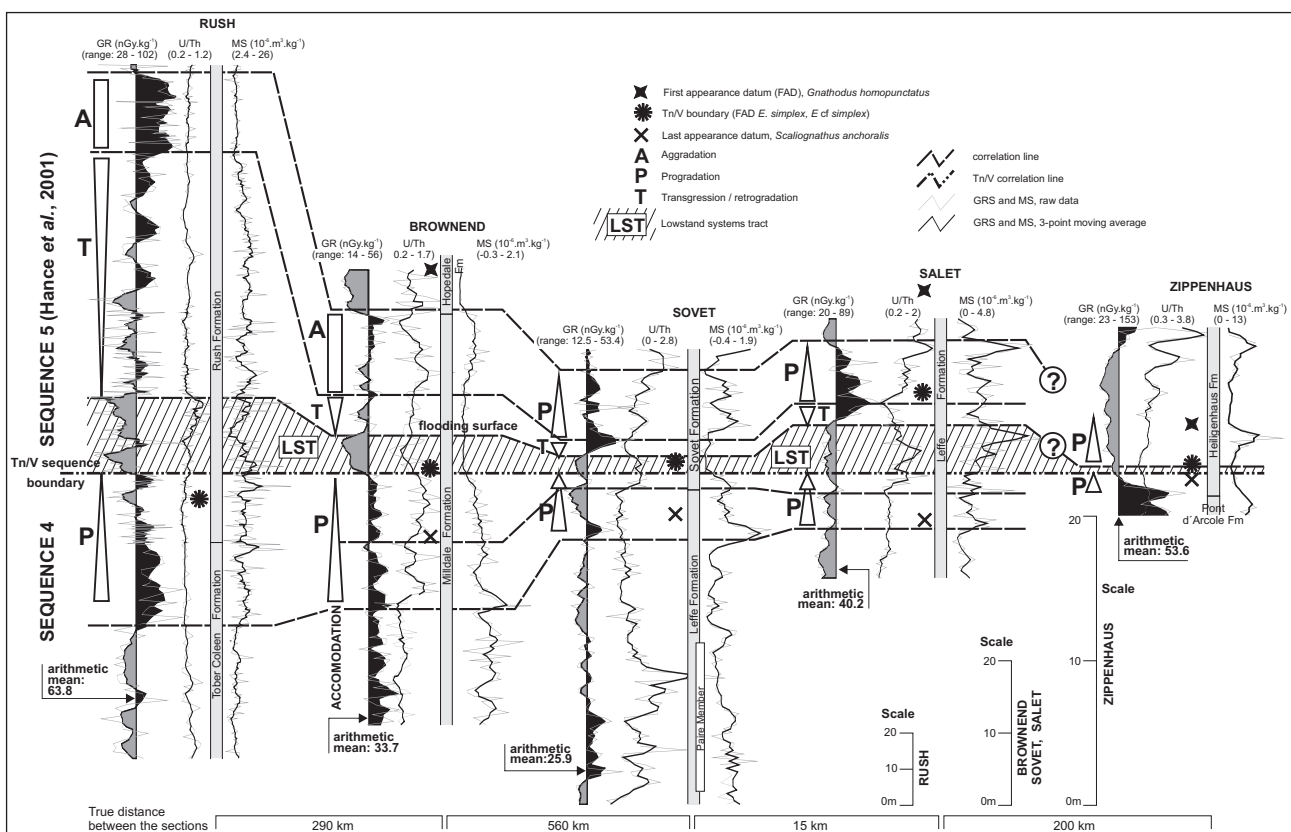


Figure 10. Correlation diagram and sequence stratigraphic interpretation of the Rush, BrownEnd, Sovet, Salet and Zippenhaus sections based on total gamma-ray (dose rate), U/Th ratios and magnetic susceptibility.

trends in Rush and Brownend, which indicate a progradation of their respective sedimentary systems (mostly turbidites). In addition, the upper Tournaisian succession between the beds 102 and 118 in Sovet coincides with the top parts of a shallowing-upward succession, which is interpreted as late highstand- and falling-stage systems tracts (Devuyst, 2006). The upper Tournaisian peaks in Th and total GR values, located close to the *Scaliognathus anchoralis* conodont zone, can be therefore interpreted as a maximum landward shift (peak transgression / maximum flooding, Ehrenberg & Svana, 2001; Ruffel et al., 2004). Up-section, there is an overall, late Tournaisian, progradation trend towards the very low GRS values at the Tn/V boundary inferred from biostratigraphy. These upper Tournaisian GRS trends also correlate with the decreasing MS values in Brownend, Sovet and Zippenhaus, which support the idea of progradation.

Negative shifts on the gamma-ray log are commonly related to basinward shifts of facies, which can be caused by a sea-level fall (Rider, 1999). Consequently, the negative GR shifts observed on top of the upper Tournaisian progradation successions (Rush, Brownend, Zippenhaus) are interpreted as sudden, basinward facies shifts due to sea-level fall (sequence boundary, Rider, 1999, cf. Sarg, 1988; Coe, 2003). The GRS minima are correlatable across all sections and occur very close to the biostratigraphically dated Tn/V boundary in most sections. The presence of the sequence boundary is supported by detailed microfacies data from bed 118 of the Sovet section (Devuyst, 2006), which coincides with the depression on the GR log. In shallow-water settings of the London-Brabant massif, exposure features and karstic surfaces in the Tn/V boundary succession are thought to indicate a regionally correlatable sea-level fall (Faulkner et al., 1990; Hance et al., 2001). Our study suggests that this important surface can be correlated to a correlative conformity in generally deep-water settings such as Brownend and Rush. The position of this sequence boundary implies that the upper Tournaisian successions in all our studied sections are correlatable with sequence 4 of Hance et al. (2001, 2002).

Above the relatively thin series of low GRS values, which are suggestive of lowstand systems tracts, there is a quick and distinct rise in the total GR values in Rush, Brownend, Sovet and Salet. It is accompanied by a drop in U/Th ratios in certain sections. Consistently with the previous assumptions, this rise is interpreted as a flooding / transgressive surface. This transgressive surface is immediately followed by a peak and then a prograding trend of decreasing total GR values in Sovet and Salet. However, in Brownend and Rush, the transgressive surface is followed by a funnel-like pattern on the GR log and consequently stable GR values, which is suggestive of a long-term retrogradation, followed by aggradation. The peak in U/Th ratios developed on the background of the generally high total GR signal in Brownend may represent a maximum flooding surface (Rider, 1999; Ruffel et al., 2004). The transgressive trend in Rush

comprises many higher-order cyclic variations, which may be related to superimposed, minor transgressive-regressive cycles. We can assume that, during the post Tn/V sea-level rise (and later highstand), the Rush depositional system was unable to prograde in a similar way as did the carbonate systems in Sovet and Salet. This could be caused by differential interplay between accommodation and supply in the two depositional systems (Schlager, 1993) or by differences in the basin configuration. Abundant turbidites and gravity-flow deposits in Rush are suggestive of a distinct shelf-to-slope geometry with well-developed shelf break and, generally, high accommodation.

In the Salet and Sovet carbonate sections, the retrogradation right above the Tn/V boundary quickly turned into progradation that lasted almost up to the top of the measured sections. From the position of the Tn/V boundary and the FAD of *Gnathodus homopunctatus* (Fig. 10) we can infer the sections on the GR logs, which are correlatable between Brownend and Salet. Hence, the retrograding-prograding section in Salet coincides with the retrograding-aggrading section in Brownend. It is suggested that limited accommodation in the source area of the Salet and Sovet successions (carbonate platform of the Condroz sedimentation area for Sovet, Waulsortian mudmounds for Salet, Hance et al., 2001) influenced the progradation of these sections during sea-level highstand higher in the Viséan (highstand shedding, Droxler & Schlager, 1985). The log differences may also reflect the different geotectonic position of Salet and Sovet (south of the London-Brabant Massif) and Brownend and Rush (north of the London-Brabant Massif) connected with the different timing of extensional pulses (Leeder, 1987).

The upper limits of the transgressive-highstand successions correlate with more-or-less prominent negative shifts on the total GR logs in the top parts of all the sections, which coincide with a rise in U/Th ratios in the Brownend, Sovet and Zippenhaus sections – patterns, which are similar to those at the Tn/V sequence boundary. It is accompanied by a drop in MS values in the pure carbonate sections of Brownend and Sovet where the MS values are generally low but the MS response is different in Rush, Salet and Zippenhaus, where the MS values are much higher. This correlatable level is assumed to represent a basinward facies shift due to the sea-level fall. It is still located beneath the FAD of *Gnathodus homopunctatus* in Brownend, Salet and Zippenhaus, while the same species is unknown from Rush and Sovet. The strong transgressive patterns immediately above the Tn/V boundary suggest that the Viséan parts of the logged sections correlate with the lower parts of depositional sequence 5 of Hance et al. (2001).

5.2 Correlation potential of magnetic susceptibility

Results from our logged sections indicate that although magnetic susceptibility can be used for long-distance correlation caution is needed (Da Silva et al., 2009 and this volume). In the pure carbonate sections such as Brownend and Sovet, the MS curves show similar shapes

while their correlation is supported by the GRS log patterns. A statistical correlation between MS values and K ($R^2 = 0.43$; Fig. 5) and Th ($R^2 = 0.32$) concentrations in Brownend suggests that the MS signal is to certain extent driven by paramagnetic, fine-grained siliciclastic admixture in the carbonates. This is supported by CU and FU facies trends close to the Tn/V boundary, which coincide with the decreasing and increasing, respectively, trends in MS in Brownend. Consistently with the K and Th trends and the facies trends, the low MS values in Brownend and Sovet are suggestive of a maximum basinward facies shift (maximum regression). In carbonate-dominated settings, the MS is thought to be related to the ratio of biogenic (carbonate, predominantly diamagnetic) to lithogenic (siliciclastic) components (Ellwood et al., 1999). Most published studies interpret the spikes and minima in MS logs in shallow-water carbonate successions as reflecting regressions and transgressions, respectively (Ellwood et al., 1999; Whalen & Day, 2009; Zhang et al., 2000, Mabillet et al., 2008). However, our result from the generally deep-water Brownend and Sovet sections suggest an opposite interpretation. During maximum regression, the MS values are low whereas during transgression and sea-level highstand, the MS values are high. Similar trends were observed by several previous authors (Da Silva et al., 2009 and this volume; Halgedahl et al., 2009; Koptíková et al., 2010). These trends are probably related to the productivity of the carbonate systems supplying carbonate to the basin. High-production systems such as rimmed-shelves show aggrading to prograding stacking patterns during relative sea level rise and highstand (keep-up systems), and subaerial exposure during sea-level lowstand. In shallow-water parts of such systems, these conditions would potentially result in spikes on MS curves during sea-level fall and low MS values during transgression and sea-level highstand.

In contrast, distal parts of low-production ramp systems and carbonate hemipelagic successions tend to develop resedimented carbonate turbidite and tempestite facies tracts during sea level lowstands (lowstand shedding) and thick retrograding successions during periods of sea level rise (Sarg, 1988; Elrick, 1996; Molina et al., 1997). Especially in distal areas, these conditions should result in low MS values during relative sea-level fall / progradation and high MS values during relative sea-level rise (transgression).

The combined MS and GRS patterns in Brownend and Sovet suggest that these successions were fed from low-productivity carbonate ramps. Problems arise in Rush, Salet and Zippenhaus where the MS values are significantly, sometimes an order of magnitude, higher than in Brownend and Sovet (Fig. 5). Here, the MS is uncorrelated with K and Th data and the MS log shapes are not correlatable between sections. We can assume that, in addition to the paramagnetic grains, which partly affect the GRS concentrations of K and Th, the high MS signal is also contributed to by ferromagnetic grains. This signal can be related to detrital or authigenic magnetic grains. However,

in order to confirm the role of minerals with different magnetic properties, additional magnetic methods would be needed, which are beyond the scope of this paper. Our results indicate that the simple low-field MS should be preferably used as a useful correlation tool in pure carbonate sections. The spectral gamma-ray logs are less sensitive to facies gradients between sections and show correlatable patterns across different lithologies. However, in favourable facies such as the Brownend section, the MS signal is much more consistent than the GRS signal, this being in all probability caused by the higher error of the GR technique (field measurement) compared to the laboratory-based MS measurements.

6. Conclusions

Gamma-ray spectrometry and, partly, magnetic susceptibility logging proved to be useful tools for the long-distance (up to ~1000 km) correlation of deep-water sections on the flanks of the London-Brabant Massif at the Tn/V boundary.

The correlatable log patterns can be interpreted in terms of relative sea-level fluctuations. An overall regressive trend in the latest Tournaisian is capped by a sequence boundary at the Tn/V boundary, which is independently indicated by biostratigraphy, lithology and published microfacies data. The overlying log patterns are interpreted as a lowstand systems tract followed by transgressive succession. The log responses above the transgressive surface vary from retrograding to aggrading and prograding in different sections, presumably due to differences in accommodation in up-dip areas. The Tn/V sequence boundary can be linked to the sea-level fall previously described from shallow-water settings and the boundary between sequence 4 and 5 of Hance et al. (2001, 2002). The combined biostratigraphic and petrophysical log correlation indicates that the sea-level fluctuations are synchronous and traceable around the Tn/V boundary on the flanks of the London-Brabant Massif.

MS signal in the Brownend deep-water carbonate section, backed by GRS and lithology data, reveals an increasing trend during transgression and a decreasing trend during regression. This response is completely opposite to the common paradigm based on the MS measurements from shallow-water carbonate platform settings (Ellwood et al., 1999; Whalen & Day, 2009; Zhang et al., 2000, Mabillet et al., 2008). We conclude that these trends are related to landward / basinward facies shifts of a low-productivity carbonate ramp system. During sea-level lowstand, carbonate tempestites and turbidites are shed into the deep water while during sea-level rise the carbonate systems backstep towards the continent, developing a retrograding succession in its distal parts (Sarg, 1988; Elrick, 1996; Molina et al., 1997, Da Silva et al., 2009 and this volume).

The GRS-based correlation between the Belgian sections Salet and Sovet is robust enough to refine the poor biostratigraphy data from the former, which is poor in foraminifers. In such a case, a GRS-based correlation is preferred. In more general terms, GRS logging has greater

correlation potential than MS as correlatable log shapes can be traced across a broad spectrum of facies and depositional settings. MS-based correlation is well-applicable in pure, thick carbonate sections but our results from a correlation between closely located and lithologically similar sections such as Salet and Sovet suggest that its use can be limited in deep-water carbonate settings.

7. Acknowledgments

This research was supported by grant project GACR 205/08/0182 (Kalvoda), GACR 205/09/1257 (Bábek) and by the research project INCHEMBIOL MSM0021622412. The reviews by Michael T. Whalen and Xavier Devleeschouwer are gratefully acknowledged.

8. References

- AMLER, M.R.W. & HERBIG, H.-G., 2006. Ostrand der Kohlenkalk-Plattform und Übergang in das Kulm-Becken im westlichsten Deutschland zwischen Aachen und Wuppertal. In Amler, M.R.W. & Stoppel, D. (eds), *Stratigraphie von Deutschland VI. Unterkarbon (Mississippium)*. Schriftenreihe der Deutschen Gesellschaft für Geowissenschaften, 41: 441-477.
- ARETZ, M., HERBIG, H.-G., & POTY, E., in print. From Palaeokarst to Calciturbidites – A carbonate platform-slope-transect from the Mississippian Limestone in eastern Belgium to the Kulm Basin in western Germany. *Kölner Forum Geologie und Paläontologie*.
- BLESS, M. J. M., BOUCKAERT, J., CONIL, R., GROESSENS, E., KASIG, W., PAPROTH, E., POTY, E., VAN STEENWINKEL, M., STREEL, M. & WALTER, R., 1980. Pre-Permian depositional environments around the Brabant Massif in Belgium, The Netherlands and Germany. *Sedimentary Geology*, 27/1: 1-81.
- COE, A.L., 2003. *The Sedimentary Record of Sea-Level Change*. The Open University and Cambridge University Press, 288p.
- COSSEY, P.J., ADAMS, A.E., PURNELL, M.A., WHITELEY, M.J., WHYTE, M.A. & WRIGHT, V.P., 2004. British Lower Carboniferous Stratigraphy. *Geological Conservation Review Series, No. 29*, Joint Nature Conservation Committee, Peterborough, 617 p.
- COSSEY, P.J., BUCKMAN, J.O. & STEWARD, D.I., 1995. The geology and conservation of Brown End Quarry, Waterhouses, Staffordshire. *Proceedings of the Geologist Association*, 106: 11-25.
- DA SILVA, A.-C., POTMA, K., WEISSENBARGER, J.A.W., WHALEN, M.T., HUMBLET, M., MABILLE, C. & BOULVAIN, F., 2009. Magnetic susceptibility evolution and sedimentary environments on carbonate platform sediments and atolls, comparison of the Frasnian from Belgium and Alberta, Canada. *Sedimentary Geology*, 214: 3-18.
- DA SILVA, A.-C., YANS, J. & BOULVAIN, F., 2010. Early-Middle Frasnian (early late Devonian) sedimentology and magnetic susceptibility of the Ardennes area (Belgium): identification of severe and rapid sea level fluctuations. *Geologica Belgica*, this volume.
- DELIUS, H., KAUPP, A., MULLER, A. & WOHLBERG, J., 2001. Stratigraphic correlation of Miocene to Plio-/Pleistocene sequences on the New Jersey shelf based on petrophysical measurements from ODP leg 174A. *Marine Geology*, 175: 149-165.
- DEVUYST, F.X., 2006. *The Tournaisian-Viséan boundary in Eurasia. Definition, biostratigraphy, sedimentology and early evolution of the genus Eoparastaffella (foraminifer)*. PhD Thesis, Catholic University of Louvain.
- DEVUYST, F.X. & KALVODA, J., 2007. Early evolution of the genus *Eoparastaffella* (Foraminifera) in Eurasia: the 'interiecta group' and related forms, late Tournaisian to early Viséan (Mississippian). *Journal of Foraminiferal Research*, 37: 1: 69-89.
- DEVUYST, F.X., HANCE, L. & POTY, E., 2006. Moliniacian. In Dejonghe, L. (ed.) Chronostratigraphic units named from Belgium and adjacent areas. *Geologica Belgica*, 9:123-131.
- DOVETON, J.H., 1994. Geologic log interpretation. *SEPM Short Course No. 29*: pp. 169
- DROXLER, A.W. & SCHLAGER, W., 1985. Glacial versus interglacial sedimentation rates and turbidite frequency in the Bahamas. *Geology*, 13: 799-802.
- EHRENBERG, S.N. & SVANA, T.A., 2001. Use of spectral gamma-ray signature to interpret stratigraphic surfaces in carbonate strata; an example from the Finnmark carbonate platform (Carboniferous-Permian), Barents Sea. *American Association of Petroleum Geologists Bulletin*, 85: 295-308.
- ELLWOOD, B.B., CRICK, R.E. & EL HASSANI, A., 1999. The magneto-susceptibility event and cyclostratigraphy (MSEC) method used in geological correlation of Devonian rocks from Anti-Atlas Morocco. *American Association of Petroleum Geologists Bulletin*, 83: 1119-1134.
- ELRICK, M., 1996. Sequence stratigraphy and platform evolution of Lower-Middle Devonian carbonates, eastern Great Basin. *Geological Society of America Bulletin*, 108: 392-416.
- FABRICIUS, I.L., FAZLADIC, L.D., STEINHOLM, A. & KORSBECH, U., 2003. The use of spectral natural gamma-ray analysis in reservoir evaluation of siliciclastic sediments: A case study from the Middle Jurassic of the Harald Field, Danish Central Graben. *Geological Survey of Denmark and Greenland Bulletin*, 2003: 349-366.
- FAULKNER, T.J., WRIGHT, V.P., PEETERS, C. & GARVIE, L., 1990. Cryptic exposure horizons in the Carboniferous Limestone of Portishead. *Avon Geological Journal*, 25: 1-17.
- FIET, N. & GORIN, G.E., 2000. Gamma-ray spectrometry as a tool for stratigraphic correlations in the carbonate-dominated, organic-rich, pelagic Albian sediments in Central Italy. *Eclogae Geologicae Helveticae*, 93: 175-181.

- FRASER, A.J. & GAWTHORPE, R.L., 1990. Tectono-stratigraphic development and hydrocarbon habitat of the Carboniferous rocks of northern England. In Hardman, R.F.P. & Brooks, J. (eds) *Tectonic Events Responsible for Britain's Oil and Gas Reserves*. Geological Society (Special Publication), 55: 49-86.
- GAWTHORPE, R.L., GUTTERIDGE, P. & LEEDER, M.R., 1989. Late Devonian and Dinantian basin evolution in northern England and North Wales. In Arthurton, R.S., Gutteridge, P. & Nolan, S.C. (eds) *The Role of Tectonics in Devonian and Carboniferous Sedimentation in the British Isles*. Yorkshire Geological Society Occasional Publication, 6: 1-24.
- HALGEDAHL, S.L., JARRARD, R.D., BRETT, C.E. & ALLISON, P.A., 2009. Geophysical and geological signatures of relative sea level change in the upper Wheeler Formation, Drum Mountains, West-Central Utah: A perspective into exceptional preservation of fossils. *Palaeogeography Palaeoclimatology, Palaeoecology*, 277: 34-56
- HANCE, L., POTY, E. & DEVUYST, F. X., 2001. Stratigraphie séquentielle du Dinantien type (Belgique) et corrélation avec le Nord de la France (Boulonnais, Avesnois). *Bulletin de la Société Géologique de France*, 172: 411-426.
- HANCE, L., POTY, E. & DEVUYST, F. X., 2002. Sequence stratigraphy of the Belgian Lower Carboniferous – tentative correlation with the British Isles. In Hills, L.V., Henderson, C.M. & Bamber, E.W. (eds) *Carboniferous and Permian of the World*. Canadian Society of Petroleum Geologists, *Memoirs*, 19: 41-51.
- HLADIL, J., GERSL, M., STRNAD, L., FRANA, J., LANGROVA, A. & SPISIAK, J., 2006. Stratigraphic variation of complex impurities in platform limestones and possible significance of atmospheric dust: a study with emphasis on gamma-ray spectrometry and magnetic susceptibility outcrop logging (Eifelian-Frasnian, Moravia, Czech Republic). *International Journal of Earth Sciences*, 95: 703-723.
- KALVODA, J., 2002. Late Devonian-Early Carboniferous foraminiferal fauna: zonations, evolutionary events, paleobiogeography and tectonic implications. *Folia Geologica*, 39, Masaryk University Brno, 213 p.
- KOPTÍKOVÁ, L., BÁBEK, O., HLADIL, J., KALVODA, J. & SLAVÍK, L., 2010. Stratigraphic significance and resolution of spectral reflectance logs in Lower Devonian carbonates of the Barrandian area, Czech Republic; a correlation with magnetic susceptibility and gamma-ray logs. *Sedimentary Geology*, 205: 83-98.
- KOPTÍKOVÁ, L., HLADIL, J., SLAVÍK, L., ČEJCHAN, P. & BÁBEK, O., 2010. Fine-grained non-carbonate particles embedded in neritic to pelagic limestones (Lochkovian to Emsian, Prague synform, Czech Republic): composition, provenance and links to magnetic susceptibility and gamma-ray logs. *Geologica Belgica*, this volume.
- KRAWCZYK, C.M. & MCCANN, T., COCKS, L.R.M., ENGLAND, R., MCBRIDE, J., & WYBRANIEC, S., 2008. Caledonian Tectonics. In McCann, T. (ed.) *The Geology of Central Europe*. Geological Society, London, 103-154.
- LEE, A. G., 1988. Carboniferous basin configuration of Central England, modelled using gravity data. In Besley, B. M. & Kelling, G. (eds), *Sedimentation in a synorogenic basin complex: the Upper Carboniferous of north west Europe*. Blackie, Glasgow: 69-84.
- LEEDER, M. R., 1987. Tectonic and palaeogeographic models for Lower Carboniferous Europe. In Miller, J., Adams, A. E. & Wright, V. P. (eds) *European Dinantian Environments*. Wiley, Chichester: 1-20.
- LÜNING, S., WENDT, J., BELKA, Z., & KAUFMANN, B., 2004. Temporal-spatial reconstruction of the early Frasnian (Late Devonian) anoxia in NW Africa; new field data from the Ahnet Basin (Algeria). *Sedimentary Geology*, 163: 237-264.
- MABILLE, C., PAS, D., ARETZ, M., BOULVAIN, F., SCHRODER, S. & DA SILVA, A.-C., 2008. Deposition within the vicinity of the Mid-Eifelian High: detailed sedimentological study and magnetic susceptibility of a mixed ramp-related system from the Eifelian Lauch and Nohn formations (Devonian; Ohlesberg, Eifel, Germany). *Facies*, 54: 597-612.
- MARCHANT, T. R., 1978. *The stratigraphy and Micropalaeontology of the lower Carboniferous (Courseyan-Arundian) of the Dublin Basin, Ireland*. Unpublished PhD Thesis, Trinity College Dublin, 420 p.
- MOLINA, J.M., RUIZORTIZ, P.A. & VERA, J.A., 1997. Calcareous tempestites in pelagic facies (Jurassic, Betic Cordilleras, Southern Spain). *Sedimentary Geology*, 109: 95-109.
- MOTTEQUIN, B. 2008. The 'black marble' of Denee, a fossil conservation deposit from the Lower Carboniferous (Visean) of southern Belgium. *Geological Journal*, 43: 197-208.
- NOLAN, S. C., 1986. *The Carboniferous geology of the Dublin area*. Unpublished PhD Thesis, Trinity College, Dublin, 319 p.
- NOLAN, S. C., 1989. The style and timing of Dinantian syn-sedimentary tectonics in the eastern part of the Dublin Basin, Ireland. In Arthurton, R.S., Gutteridge, P. & Nolan, S.C. (eds) *The Role of Tectonics in Devonian and Carboniferous Sedimentation in the British Isles*. Yorkshire Geological Society Occasional Publication, 83-97.
- POTY, E., DEVUYST, F.X. & HANCE, L., 2006. Upper Devonian and Mississippian foraminiferal and rugose coral zonations of Belgium and Northern France: a tool for Eurasian correlations. *Geological Magazine*, 143: 829-857.
- RIDER, M.H., 1999. *The Geological Interpretation of Well Logs*. Whittles Publishing Services, 288 p.

RUFFEL, A. & WORDEN, R., 2000. Palaeoclimate analysis using spectral gamma-ray data from the Aptian (Cretaceous) of southern England and southern France. *Palaeogeography Palaeoclimatology, Palaeoecology*, 155: 265-283.

RUFFEL, A., MCKINLEY, J.M. & EVANS, R., 2004. Distinguishing faults from flooding surfaces on spectral gamma-ray logs. *American Association of Petroleum Geologists Bulletin*, 88: 1239-1254.

SARG, J.F., 1988. Carbonate sequence stratigraphy. In Wilgus, C.K., Hastings, B.S., Kendall, C.G.S.C., Posamentier, H.W., Ross, C.A. & Van Wagoner, J.C. (eds) *Sea-Level Changes: An Integrated Approach*. SEPM Special Publication, 42: 155-182 .

SCHLAGER, W., 1993. Accommodation and supply - a dual control on stratigraphic sequences. *Sedimentary Geology*, 86: 111-136.

SEVASTOPULO, G. D. & WYSE JACKSON, P.N., 2008. Carboniferous: Mississippian (Tournaisian and Viséan). In Holland, C.H. & Sanders, I.S. (eds) *The Geology of Ireland*. 2nd Revised edition, Dunedin Academic Press, 568 p.

SIEGMUND, H., TRAPPE, J. & OSCHMANN, W., 2002. Sequence stratigraphic and genetic aspects of the Tournaisian "Liegender Alaunschiefer" and adjacent beds. *International Journal of Earth Sciences*, 91: 934-949.

TAKANO, S., ITO, M., NAKANO, T., HORIKAWA, K., NAKAMURA, Y. & SAITO, T., 2004. Sequence-stratigraphic signatures of hemipelagic siltstones in deep-water successions: the Lower Pleistocene Kiwada and Otadai formations, Boso Peninsula, Japan. *Sedimentary Geology*, 170: 189-206.

THIBAL, J., ETCHECOPAR, A., POZZI, J.P., BARTHES, V. & POCACHARD, J., 1999. Comparison of magnetic and gamma ray logging for correlations in chronology and lithology: example from the Aquitanian Basin (France). *Geophysical Journal International*, 137: 839-846.

WATERS, C.N., WATERS, R.A., BARCLAY, W.J. & DAVIES, J.R., 2009. *A lithostratigraphical framework for the Carboniferous successions of southern Great Britain (Onshore)*. Nottingham, UK, British Geological Survey, 185 p.

WHALEN, M.T. & DAY, J.E., 2009. Magnetic susceptibility, biostratigraphy, and sequence stratigraphy: insights into Devonian carbonate platform development and basin infilling, Western Alberta, Canada. In Lukasik, J. & Simo, J.A. (eds) *Controls on carbonate platform and reef development*. SEPM Special Publication, 89: 291-314

ZHANG, S.H., WANG, X.L. & ZHU, H., 2000. Magnetic susceptibility variations of carbonates controlled by sea-level changes - Examples in Devonian to Carboniferous strata in southern Guizhou Province, China. *Science in China Series D-Earth Sciences*, 43: 266-276.

ZIEGLER, P. A., 1982. *Geological Atlas of Western and Central Europe*. Shell B.V., 130 p.

Manuscript received 05.12.2009, accepted in revised form 27.04.2010, available on line 25.06.2010.

